ORIGINAL PAPER

Estimating return periods for daily precipitation extreme events over the Brazilian Amazon

Eliane Barbosa Santos[1] · Paulo Sérgio Lucio[1] · Cláudio Moisés Santos e Silva[1]

Abstract This paper aims to model the occurrence of daily precipitation extreme events and to estimate the return period of these events through the extreme value theory (generalized extreme value distribution (GEV) and the generalized Pareto distribution (GPD)). The GEV and GPD were applied in precipitation series of homogeneous regions of the Brazilian Amazon. The GEV and GPD goodness of fit were evaluated by quantile–quantile (Q-Q) plot and by the application of the Kolmogorov–Smirnov (KS) test, which compares the cumulated empirical distributions with the theoretical ones. The Q-Q plot suggests that the probability distributions of the studied series are appropriated, and these results were confirmed by the KS test, which demonstrates that the tested distributions have a good fit in all sub-regions of Amazon, thus adequate to study the daily precipitation extreme event. For all return levels studied, more intense precipitation extremes is expected to occur within the South sub-regions and the coastal area of the Brazilian Amazon. The results possibly will have some practical application in local extreme weather forecast.

1 Introduction

The Brazilian Amazon is located in the equatorial region between 5° N–18° S and 42° W–74° W. The climate of this region is related to the performance of meteorological phenomena at different scales, modulated by ocean–atmosphere

mechanisms, which produce total rainfall above and/or below the climatological average. The topography and the local circulation are also important in this region and can increase the activity of convective systems, which under favorable weather conditions can cause heavy rainfall and severe weather in a few hours (Smith et al. 1996).

Climate is generally defined as average weather, and as such, climate change and weather are intertwined. To understand the causes of daily precipitation extreme events, such as floods, we must have knowledge of the causes of rainfall phenomena in the region. In the synoptic scale, the main meteorological systems that modulate rainfall in the Amazon are (i) Intertropical Convergence Zone (ITCZ), the main system that modulate rainfall variability in the Amazon coast, responsible for the maximum precipitation during the austral autumn (De Souza et al. 2005; De Souza and Rocha 2006) and (ii) the South Atlantic Convergence Zone (SACZ), which operates mainly in the Southern and Southwest region of the Amazon, and are responsible for the maximum precipitation by the end of austral spring and summer (Carvalho et al. 2004; Grimm 2011; De Oliveira Vieira et al. 2013).

As for the meso-scale systems, it is highlighted that the Coastal Squall Lines (CSL) (Cohen et al. 1995) are formed along the north and northeast coast of South America, associated with sea breeze circulation, more frequent between April and June and less frequent between October and November (Alcantara et al. 2011). Besides, the local wind mechanisms, such as river breeze, are also important to the diurnal cycle and the intensity of the rainfall in this region (Oliveira and Fitzjarrald 1993; Silva Dias et al. 2004).

The beginning of the XXI century has been marked by a diverse series of extreme events of precipitation over the Amazon (Marengo et al. 2008a, b, 2011; Vale et al. 2011; Sena et al. 2012; Coelho et al. 2012). According to Gloor et al. (2013), since 1990 there is an intensification of the Amazon

✉ Eliane Barbosa Santos
  elianbs@gmail.com

[1] Programa de Pós-graduação em Ciências Climáticas, Universidade Federal do Rio Grande do Norte, Campus Universitário Lagoa nova, caixa postal 1524, Natal, Rio Grande do Norte ZIP 59078-970, Brazil

hydrological cycle, with an increase of drainage during the rainy season and eventual severe droughts. Langerwisch et al. (2013) have studied the effects of climatic changes on the flood regime of the Amazon Basin. These authors have used the Dynamic Global Vegetation and Hydrology Model LPJmL, enhanced by a scheme that realistically simulates monthly flooded area. The results show an increase in duration and in the area of inundation, in around one third of the basin.

The intense precipitation events have caused a major impact on the socioeconomic activities of the Amazon, making the population vulnerable to the behavior and variability of the climate system. In 2014, two states of the Brazilian Amazon (Acre and Rondônia) declared a state of calamity due to floods caused by heavy rainfall in the headwaters of the rivers. In this context, the probabilistic prediction of occurrence of extreme precipitation events is of vital importance for the planning of activities exposed to its adverse effects. One way to model these events is use the extreme values theory (EVT), through the generalized extreme value (GEV) distribution, which includes the distributions of Gumbel, Fréchet, and Weibull and generalized Pareto distribution (GPD) as the exponential, Pareto and Beta.

The EVT models the extremes using the distribution of maximum or minimum and the excess. In the study of the maximum or minimum, the sample is divided in sub-periods (blocks) that may be monthly, annually, etc. From each block, a maximum or minimum value is extracted, to compose a set of extreme data, according to the block maximum methodology, associated to the GEV distribution (Maraun et al. 2009; Sugahara et al. 2009). The exceeding values are determined according to the adopted limit, in accordance with the picks over threshold methodology, associated to the GPD (Sugahara et al. 2009).

The EVT was first developed by Fisher and Tippett (1928) and formalized by Gnedenko (1943). Significant contributions to the statistical modeling of extremes were published by Jenkinson (1955) for GEV and Pickands (1975) for GPD. In comparison with the long history of theoretical results of EVT, the empirical analysis of precipitation data using EVT is relatively new. Application of GEV and GPD to rainfall data are found in the last two decades in several publications (Withers and Nadarajah 2000; Li et al. 2005; Bordi et al. 2007; Nadarajah and Choi 2007; DeGaetano 2009; Barbara et al. 2010; Ender and Ma 2014).

It is important that the meteorological risks that we are exposed be correctly evaluated and dimensioned, since the increase of economic losses due to extreme weather and especially the increase of deaths has been constantly in newspaper reports (Kostopoulo and Jones 2005). Thus, the objective of this paper is to model the occurrence of intense precipitation events in the Brazilian Amazon and estimate the return period of such events through EVT (GEV and GPD), indicating the regions with worse occurrences.

2 Material and methods

2.1 Datasets

Daily precipitation dataset was obtained from the National Water Agency (*Agência Nacional de Água* (ANA)) and Bank of Meteorological Data for Education and Research (*Banco de Dados Meteorológicos para Ensino e Pesquisa* (BDMEP)) of the National Institute of Meteorology (*Instituto Nacional de Meteorologia* (INMET)). The rain gauges were selected following the recommendations of the World Meteorological Organization (WMO), established in Technical Document WMO-TD/No. 341 for the period from 1983 to 2012. In this document, it is recommended to (i) discard the month that shows any missing daily value and (ii) exclude the climatological normal monthly data that present three or more consecutive days of missing observations or more than five alternate months missing. The initial set consisted of 1129 rain gauges, but following the recommended WMO procedure, 305 remained.

2.2 Methods

The return period of the extreme precipitation events in the Brazilian Amazon was obtained for homogeneous rainfall regions, determined by Santos et al. (2014). These authors have used Ward's hierarchical clustering method and as similarity measure, the Euclidian distance. Six homogeneous subregions were identified (Fig. 1): two sub-regions of Southern Brazilian Amazon; four sub-regions up North, being two in the coastal area and two in the Northwest portion. The associated meteorological systems responsible for the observed rainfall in these regions will be discussed in Sect. 3.

According to Santos et al. (2014), these sub-regions are sufficient to represent the precipitation in the Brazilian Amazon. In this present paper, synthetic series of precipitation were used, which consists in using the daily maximum values of each sub-region, i.e., the synthetic series was formed by data from different stations for different days. As the extreme precipitation events can occur in any season, the analyzes were performed with the complete series, i.e., the precipitation series were not separated by season or months.

The synthetic series were analyzed considering the EVT, which is a branch of theoretical probability that studies the stochastic behavior of the extremes associated to a distribution function F, normally unknown. This theory deals essentially with the asymptotic distributional behavior of two types of data, namely, the so-called block maxima and peaks over threshold. The first type refers to the maximum values extracted from blocks (subsets) of observations, whereas the second type refers to observations that exceed a given threshold.

Fig. 1 Spatial distribution of stations used in this study for the six homogeneous rainfall regions of the Brazilian Amazon (R1, R2, R3, R4, R5, and R6). Source: Adapted from Santos et al. (2014)
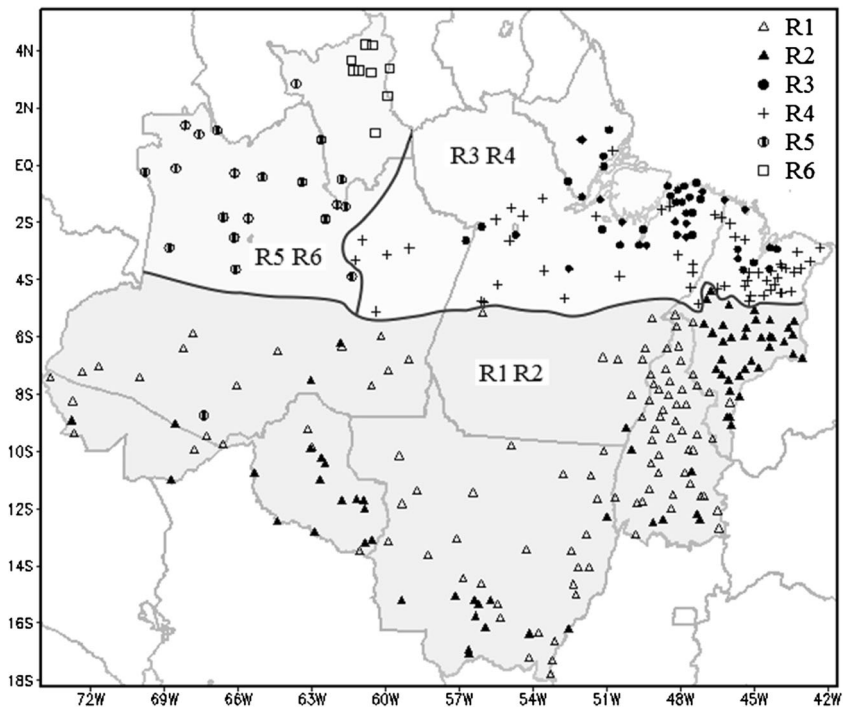
Coles (2001) demonstrates the initial formulation of the model as follows:

$$M_n = \max\{x_1, ... x_n\} \tag{1}$$

where M_n is the maximum of n units, and $x_1, ... , x_n$ a sequence of independent random variables identically distributed with cumulative distribution F in common.

The exact distribution function of the maximum can be obtained for all values of n, as follows:

$$F_{M_n(x)} = P(M_n \leq x) = P(X_1 \leq x, ..., X_n \leq x) = (F_X(x))^n \tag{2}$$

Since F is unknown, a way of knowing it is to seek families of models next in the F^n distributions. The idea is similar to the approach procedure of the distribution of sample means in normal distribution, according to the central limit theorem.

The EVT is analogous to the central limit theorem but applies to large deviations or extremes. Moreover, the central limit theorem provides a unique limit of distribution, while EVT includes three different families of asymptotic distributions. Its main goal is to stimulate the upper tail of a probability distribution function of a set of independent and identically distributed observations. The extreme precipitation events can occur in any season or occur predominantly in a season. Then, to ensure the independence of the temporal series of daily precipitation and remove the seasonal dependency, the values were randomized. Thus, if extreme events occur in only one season, with randomization, these events become random.

To test the hypothesis of independence of data, the non-parametric test of sequences of adherence to the normal distribution, called runs tests, which checks whether the elements of the series are independent of each other was used. A 5 % significance level was adopted for the test. According to Sharma et al. (1999), the implementation of this assumption ensures the achievement of satisfactory statistical inferences from probabilistic models of extreme values.

To verify the quality of the parameters from the EVT distributions, the quantile–quantile (Q-Q) plot will be analyzed, since it is one of the most used methods in the verification for fitting the theoretical distribution to the empirical one, consisting in the graphical comparison of theoretical quantiles of the distribution, with the quantiles of sample data, showing the relationship between the fitted and the observed data.

However, the graphical methods are subject to mistakes, once they depend on the visual interpretation. For a more objective result, a non-parametric test was used—the Kolmogorov–Smirnov (KS) test (Chakravarti et al. 1967). In the KS test, the following null hypothesis is considered $H_0 : F(x) = G(x)$ and the alternative hypothesis is $H_1 : F(x) \neq G(x)$. The test statistic is obtained by $D_n = \sup_x |F(x) - G_n(x)|$, where $F(x)$ is the theoretical cumulative distribution function and $G(x)$ is the empirical cumulative distribution function, to n random observations with a cumulative distribution function. This test represents the upper extreme limit of differences between absolute values of the empirical and theoretical cumulative distribution considered in the test (Lucio 2004). The null hypothesis is rejected if the D_n value is greater than the tabulated one. This is equivalent to consider that the exact probability of the test is lower than the significance level. Hence, the KS test was

applied to compare the goodness of fit of the GEV and GPD distributions, with a significance level of 5 %.

In this study, we have employed EVT distribution, considering GEV and GPD, to model the maximum and rainfall excesses, respectively. In this theory, the return period (or the average recurrence interval) is corresponding to the probability p of a return level has $p100$ % chance of being exceeded in a given year. The concepts of return level and return period are commonly used to convey information about the likelihood of rare events such as floods. A return level with a return period of $T = 1/p$ years is a high threshold x_P (e.g., annual peak flow of a river) whose probability of exceedance is p.

2.3 Generalized extreme values distribution

The GEV distribution function combines three asymptotic forms of extreme value distributions, Gumbel, Weibull and Fréchet (Fisher and Tippett 1928), in a unique form, defined according to Jenkinson (1955) as follows:

$$F(x) = \exp\left[-\left(1-\xi\frac{x-\mu}{\sigma}\right)^{\left(\frac{1}{\xi}\right)}\right], \text{if } \xi{\neq}0 \qquad (3a)$$

$$F(x) = \exp\left[-\exp\left(-\frac{x-\mu}{\sigma}\right)\right], \text{if } \xi = 0 \qquad (3b)$$

where μ is the location parameter $-\infty<\mu<\infty$; σ is a scale parameter $0<\sigma<\infty$; and ξ is the shape parameter with $-\infty<\xi<\infty$.

The extreme value distribution of Weibull and Fréchet corresponds to the particular cases of (3a) in where $\xi < 0$ and $\xi > 0$, respectively. When $\xi = 0$, the function assumes a form (3b), which represents a Gumbel distribution.

For the quantile x_P of GEV distribution, with the return period T, the cumulated probability is given by $F(x_P)=1-(1/T)$, which results in (Palutikof et al. 1999):

$$x_p = \mu + \frac{\sigma}{\xi}\left[1-\left(-\ln\left(1-\frac{1}{T}\right)\right)^{\xi}\right], \text{if } \xi{\neq}0 \qquad (4a)$$

$$x_p = \mu-\sigma\ln\left[-\ln\left(1-\frac{1}{T}\right)\right], \text{if } \xi = 0 \qquad (4b)$$

In GEV distribution, the sample is divided in sub-periods (blocks) that may be monthly, seasonal or annual, etc. From each block, a maximum or minimum value is extracted, to compose a set of extreme data, according to the block maximum methodology, or annual maximums (Gumbel) (Maraun et al. 2009; Sugahara et al. 2009). In this study, in the GEV distribution, the annual maximums were considered as extremes, through the block maxima method. As the study period is from 1983 to 2012 (30 years), the final dataset consists in 30 observations of annual maximums of precipitation.

2.4 Generalized Pareto distribution

Pickands (1975) has showed that the asymptotic distribution of excesses of a random variance above a threshold value may be approximated by GPD (peaks over threshold approach). As GEV, the GPD may be understood as a family of distributions that, depending on the parameter value of the form, includes particular cases, defined as:

$$F(x) = 1-\left(1-\frac{\xi}{\sigma}(x-u)\right)^{-\frac{1}{\xi}}, \text{if } \xi{\neq}0 \qquad (5a)$$

$$F(x) = 1-\exp\left(-\frac{(x-u)}{\sigma}\right), \text{if } \xi = 0 \qquad (5b)$$

where u is the selected threshold, or in other words, the values of $x - u$ are the exceeds. For $\xi = 0$, the GPD is an exponential distribution. For $\xi > 0$, the GPD is the Pareto distribution, and for $\xi < 0$, the GPD is the Beta distribution.

The quantile x_P of GPD will be found as follows (Abild et al. 1992; Palutikof et al. 1999):

$$x_p = u + \frac{\sigma}{\xi}\left[1-(\lambda T)^{-\xi}\right], \text{if } \xi{\neq}0 \qquad (6a)$$

$$x_p = u + \sigma\ln(\lambda T), \text{if } \xi = 0 \qquad (6b)$$

Where λ is equal to $\frac{n}{M}$, where n is the total number of excesses over the threshold u and M is the number of years of the registry.

In GPD, the datasets was determined according to the picks over threshold methodology, which considers only the values above the established threshold (Sugahara et al. 2009). The threshold indicates the minimum value of the extremes selected for each sub-region. There were some problems in choosing the threshold because very high thresholds increase uncertainty in the sample (variance) associated with the estimated quantile. At the same time, very low thresholds tend to increase the quantile bias. Thus, it is expected that an optimal threshold is found, to minimize both the bias and the variance (An and Pandey 2005), and in this study, we found good thresholds.

The threshold was defined based on the calculation of the quantiles of the distribution of precipitation. Testing the quantiles above 95 % in the complete series (1983–2012), the best goodness of fit of the GPD was found using quantile 99.7 % as the threshold. Then we selected the 0.3 % of data located in the upper end of each distribution, corresponding to 32 observations of extremes in each sub-region. To confirm the choice of an appropriate threshold, the method proposed by Davison and Smith (1990) was used, which consists in a choice of a threshold by the analyses of the mean excess plot, as illustrated in Fig. 3.

The estimate of distribution parameters from the GEV (μ, σ, and ξ) and from the GPD (σ and ξ) was made by the maximum likelihood method (Smith 1985).

3 Results and discussion

Figure 2 shows the box plot of daily precipitation throughout the year for the six sub-regions. The sub-regions of the Southern Brazilian Amazon (R1 and R2) have similar patterns and were separated due to intensity of precipitation. Precipitation of R2 is less intense compared with R1. The intensity of precipitation of these sub-regions may be related to the kinds of vegetations, as well as deforestation areas (Durieux et al. 2003) or can be attributed also to natural factor such as topography.

The results found by Bagley et al. (2014) suggest that the deforestation has a potential of increasing the impact over drought in the Amazon Basin. According to Durieux et al. (2003), there are significant changes in the characteristics of clouds covering deforested areas, considering the seasonal variations. During the dry season, there is less convection during the night and the early morning, leading to few precipitations. During the rainy season, the convection is stronger in the beginning of the night, leading to higher precipitation. However, we did not perform statistical analyses in order to verify the relationship between deforestation and rainfall over these regions during the studied period (1983–2012). In this sense, precipitation variability in the sub-regions R1 and R2 is here attributed to natural factors such as topography.

Figure 2a, b shows that in R1 and R2, the highest precipitation values are found by the end of spring and austral summer. These results are in accordance with Marengo and Nobre (2009) and are attributed to the manifestation of the SACZ during this period (Carvalho et al. 2004; Grimm 2011. De Oliveira et al. 2013).

The sub-regions R3 (Amazon coast) and R4 (central region of Pará States, east Amazonas States, and southern Maranhão States), are also separated by the precipitation intensity. The rain distribution in these sub-regions is related to the ITCZ. According to De Souza et al. (2005) and De Souza and Rocha (2006), the ITCZ is responsible for the maximum precipitation during the austral autumn, as illustrated in Fig. 2c, d. Another important system is the CSL (Cohen et al. 1995; Alcantara et al. 2011) but not every CSL propagates inland to the Amazon away from the coast. This is apparently the reason why precipitation in R4 is less intense when compared with R3, although the evidence shown in Fig. 2c, d does not clearly indicate large differences between R3 and R4 daily precipitation.

The R6 sub-region of Northwest Amazon is formed by stations of Roraima State, which are all located in the Northern Hemisphere, presents climate features of the North Hemisphere, with maximum precipitation during the austral winter, as previously documented by Rao and Hada (1990) and Reboita et al. (2010). The maximum precipitation during the austral winter is related to the ITCZ, which is located north of the equator in the Northern Hemisphere summer (austral winter). In R5, in the Northwest and Nor-Northwest Amazon state, precipitation is evenly distributed during all months of the year, not showing a well-defined dry period. The precipitation in this sub-region can be explained in terms of the condensation of moist air transported by the trade winds and lifted because of the influence of the Andes (Nobre et al. 1991; Garreaud and Wallace 1997; Da Rocha et al. 2009).

The outliers (circles outside the whiskers of the box plots in Fig. 2), which are considered extreme precipitation events, were seen in all sub-regions and in all months. However, it
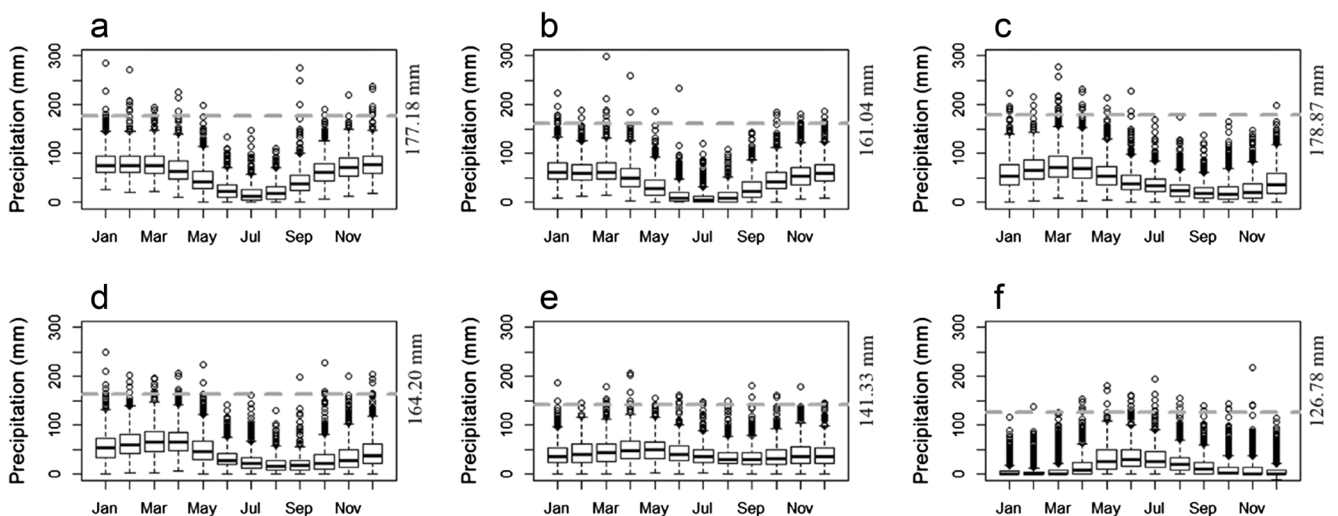

Fig. 2 Box plot of the daily precipitation in all months of the year for homogeneous rainfall regions of the Brazilian Amazon: **a** R1, **b** R2, **c** R3, **d** R4, **e** R5, and **f** R6. The *gray-dashed lines* represent the 99.7th percentile

is noted in Fig. 2 that the series belonging to R5 and R6 present mean values less elevated, with outliers presenting less intense precipitation. The R5, region of northwest and Nor-Northwest Amazon state, presents high precipitations during all year, but since the averages and medians in all months were lower than 50 mm, more than 50 % of its values are lower than 50 mm.

In the EVT, the observations have to be independent and identically distributed. Hence, the second phase of the study was to verify through the runs test, the assumption of independency of observations, to estimate the parameters of GEV and GPD distributions. With the run test, it was verified that temporal series of all sub-regions have made through the random test after being ungrouped.

In the GPD distribution, the adopted thresholds (μ) in each sub-region were found using quantile 99.7 % as threshold. As verified by the box plot analysis (Fig. 2), the sub-regions with extreme values less elevated were R5 and R6, with thresholds of 141.33 and 126.78 mm, respectively.

With the intention to confirm the choice of adequate threshold, the mean excess plot as a function of chosen thresholds was also analyzed (Fig. 3). Figure 3 shows that for R1, R2, R3, and R4 thresholds around 150 mm or higher may be adopted. However, for R5 and R6 lower thresholds from around 100 mm may be adopted, in agreement with the obtained threshold values using the 99.7th percentile. In Fig. 3, the change of inclination indicates different parameters for the distribution (GPD) and the irregular behavior in the right side of the figure is due to the small number of exceed above high thresholds.

After verifying the independence assumption of observations and choosing the thresholds of GPD, we have estimated the GEV and GPD distribution parameters with the maximum likelihood method, for each sub-region (Figs. 4 and 5). The estimated parameter of shape (ξ) is within −0.5 and 0.5 and,

thus, it may be applied to the method (Smith 1985). According to Smith (1985), the regularity conditions for estimation by the maximum likelihood estimation are not necessarily satisfied when $-1 \le \xi \le -0.5$. In these cases, the maximum likelihood estimators exists but do not satisfy the conditions of regularities. When $\xi < -1$, the maximum likelihood estimators do not exist.

In the GEV distribution (Fig. 4), it is noted that in the R1 and R4, the estimated parameter of shape (ξ) are higher than zero. In R2 and R3, they were equal to zero and in R5 and R6, lower than zero, corresponding to Fréchet, Gumbel, and Weibull distribution, respectively. The standard error estimates of the distribution parameters are between 3.64 (R4) and 6.59 (R1) for the location parameter, 2.97 (R5) and 5.43 (R1) for the scale parameter, and 0.12 (R2 and R5) and 0.26 (R1) for the shape parameter.

In GPD (Fig. 5), the estimative of parameter of shape (ξ) in R5 is higher than zero, corresponding to the Pareto distribution, and in R3, R4, and R6, correspond to Beta, because the estimates were for values lower than zero. In R1 and R2, they were equal to zero, corresponding to the exponential distribution. The standard error estimates for the shape parameter were similar to the ones obtained in the GEV distribution, between 0.15 (R3) and 0.25 (R1 and R5). For the scale parameter, standard error estimates were higher in the GPD, between 4.03 (R5) and 8.38 (R1).

Table 1 shows daily precipitation extreme events return periods in six sub-regions obtained from the GEV and GPD fits shown in Figs. 4 and 5, respectively. The results obtained using the GEV distribution (Fig. 4) were similar to the ones obtained using the GPD distribution (Fig. 5). These results suggest that on average, at least once a year daily precipitation equal to or higher than 152.1, 144.6, 164.6, 149.7, 120.0, and 97.9 mm are registered in the six investigated regions, and at least once every 10 years, a total equal to or higher than 246.7,
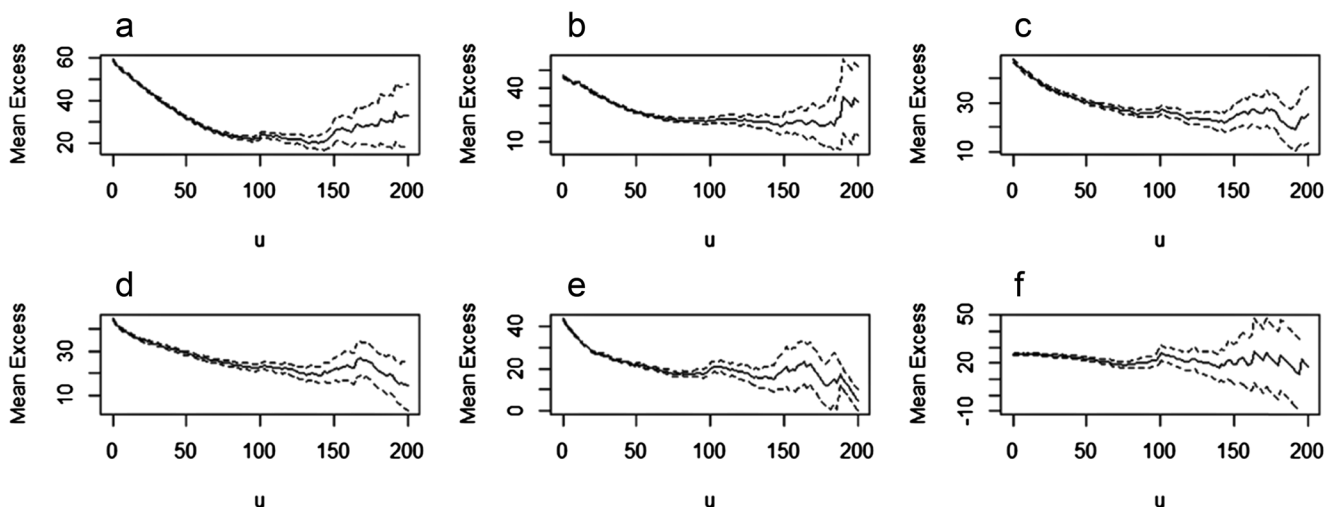

Fig. 3 Mean excess plot. Thresholds μ (mm) vs mean excess of the daily precipitation (mm) for homogeneous rainfall regions of the Brazilian Amazon: **a** R1, **b** R2, **c** R3, **d** R4, **e** R5, and **f** R6. The dashed lines represent 95 % confidence intervals
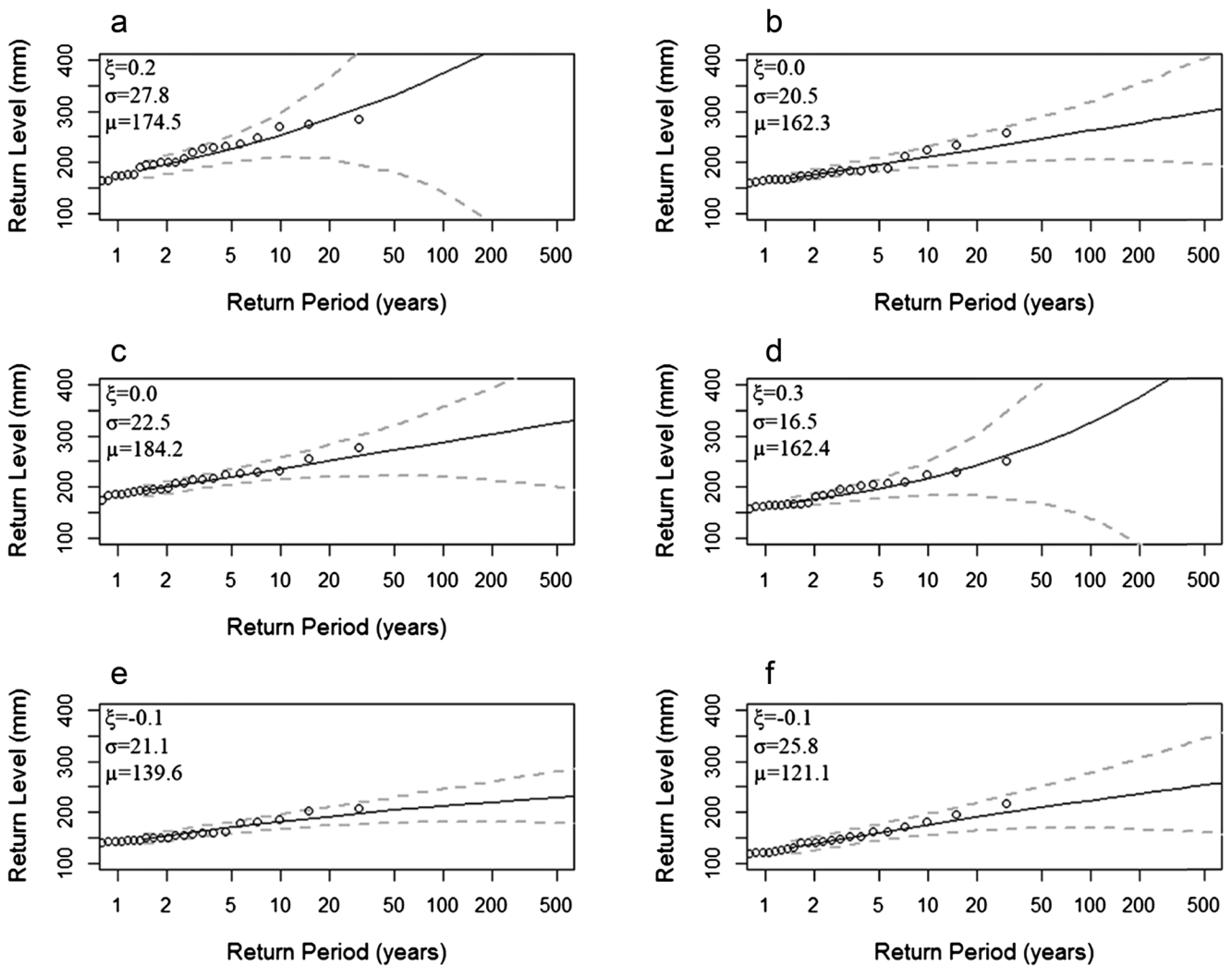
Fig. 4 Return period of extreme precipitation events with its respective parameters GEV (μ, σ, and ξ) for homogeneous rainfall regions of the Brazilian Amazon: **a** R1, **b** R2, **c** R3, **d** R4, **e** R5, and **f** R6. The *gray lines* represent 95 % confidence intervals, and the *central black line* is the estimated model. The *open circles* are observed values

209.8, 234.9, 215.3, 180.3, and 175.1 mm are registered in these six regions.

The lower values of the extremes of daily precipitations were found in R5 and R6, located in the Northwest of Amazon. This result is consistent with Fig. 2, which shows that these sub-regions present the lowest outliers with reduced precipitation intensity compared with the other investigated regions. However, the two greatest floods in these regions occurred during the manifestation of La Niña (2009 and 2012) when the South Tropical Atlantic Ocean was abnormally warm. Due to sea surface temperatures anomalies of the South Tropical Atlantic, the ITCZ remains longer in the South in comparison with its normal behavior, leading to extreme rains in the Amazon (Marengo et al. 2012b, 2013).

The events of greater daily precipitation intensity were found in R1 and R3. R1 belongs to the Southern Amazon and is influenced by the Monsoon System in South America (Marengo et al. 2012a), which controls the formation of SACZ (Zhou and Lau 1998), and its spatial and temporal variability has a fundamental role for the distribution of extreme rainfall in these regions (Carvalho et al. 2002, 2004). In the same way, R2 also appears with important daily precipitation extreme events, but of lower intensity when compared with R1, once most of its stations are located in transition regions, where one can find the *cerrado* vegetation, such as southern Maranhão. Comparing the R3 and R4, the highest precipitation in R3 is explained by the proximity of these data collection points to the coast.

To verify the goodness of fit for GEV and GPD, Figs. 6 and 7 must be analyzed, which represent Q-Q plot for the fitted distribution of GEV and GPD, respectively. The figures show that most of the points of Q-Q plot are located near the diagonal (45°) line, suggesting that the chosen and fitted theoretical distributions are
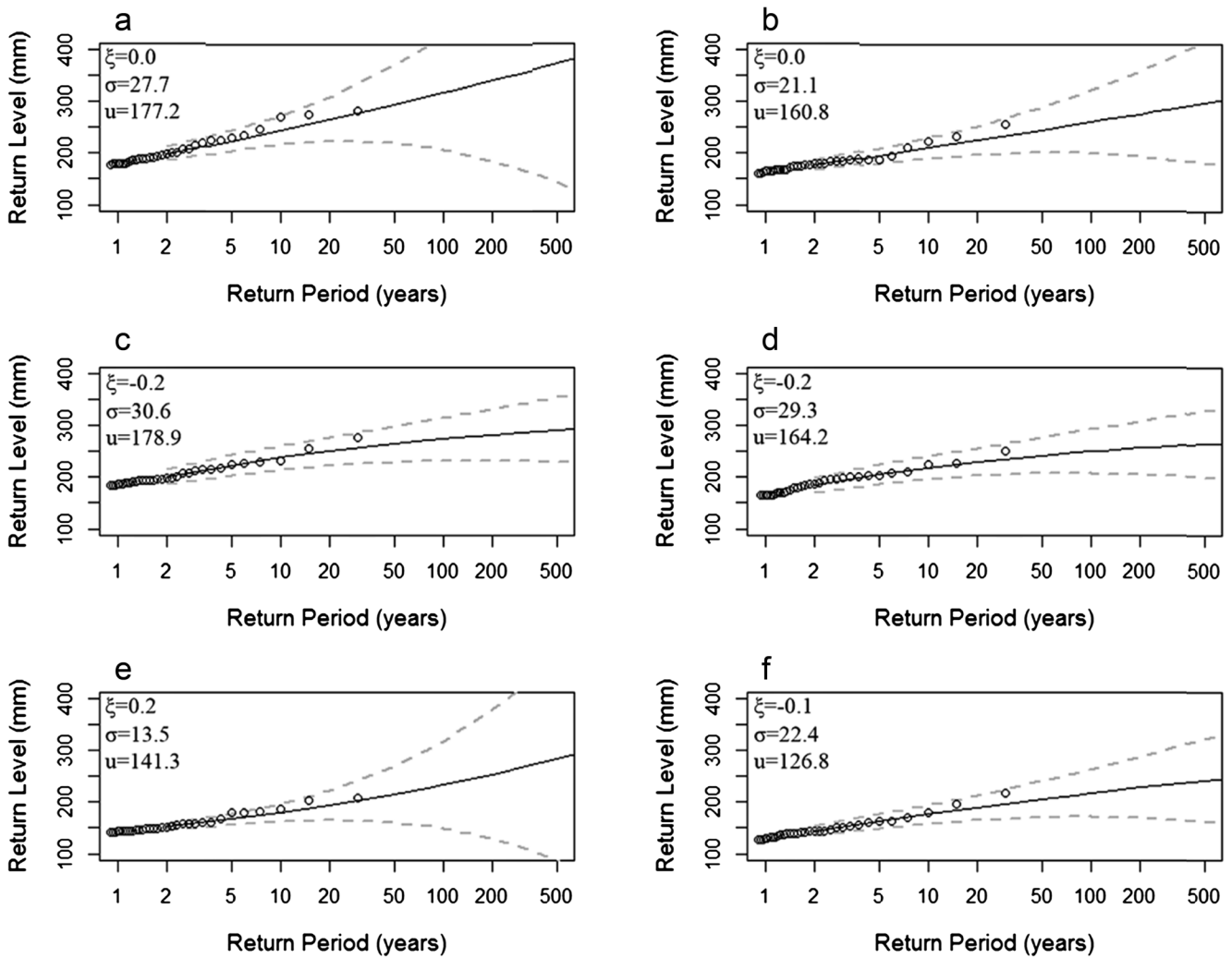
Fig. 5 Return period of extreme precipitation events with its respective parameters GPD (σ and ξ) and thresholds (μ) for homogeneous rainfall regions of the Brazilian Amazon: **a** R1, **b** R2, **c** R3, **d** R4, **e** R5, and **f** R6. The *gray lines* represent 95 % confidence intervals, and the *central black line* is the estimated model. The *open circles* are observed values

appropriate. To further support these results, the KS test was calculated (Table 2).

In this study, we have 30 observations of annual maximums of precipitation (GEV distribution) and 32 observations excesses above the adopted 99.7th percentile threshold (GPD distribution). For samples between 30 and 34 observations,

the critical value D_n used in the KS test is 0.24, which corresponds to the significance level of 5 %. In Table 2, it is possible to observe the results of the test, indicating that GEV and GPD distributions were accepted with 5 % of significance in all sub-regions, with more adequate results in the GEV distribution.

Table 1 Return level (mm) for the six sub-regions of the Brazilian Amazon, for different return periods (in years), obtained through GEV and GPD distributions

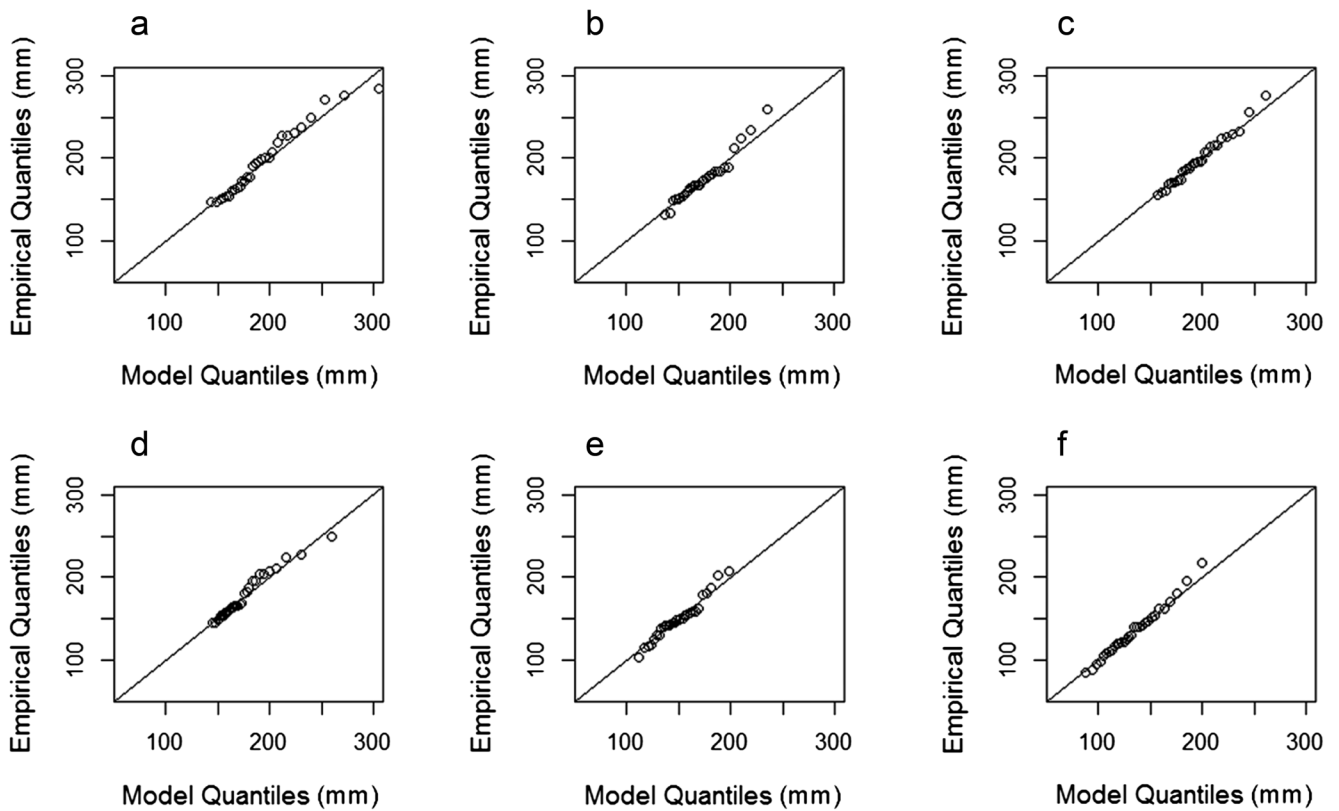|	GEV					GPD				
	1	5	10	50	100	1	5	10	50	100
R1	152.1	222.3	251.5	331.6	373.26	179.8	225.9	246.7	296.8	319.3
R2	144.6	193.6	209.8	246.3	262.3	162.8	197.1	212.0	247.2	262.5
R3	164.6	217.9	234.9	272.1	287.9	181.7	223.5	237.9	264.9	274.2
R4	149.7	193.6	215.3	284.4	325.6	166.1	205.3	218.3	242.1	250.6
R5	120.0	168.4	180.8	204.4	212.9	142.6	167.5	180.3	215.7	233.8
R6	97.9	158.0	175.1	209.7	223.2	128.9	162.9	176.5	205.7	217.3

Fig. 6 Quantile–quantile plot for the fit of GEV distribution for homogeneous rainfall regions of the Brazilian Amazon: **a** R1, **b** R2, **c** R3, **d** R4, **e** R5, and **f** R6
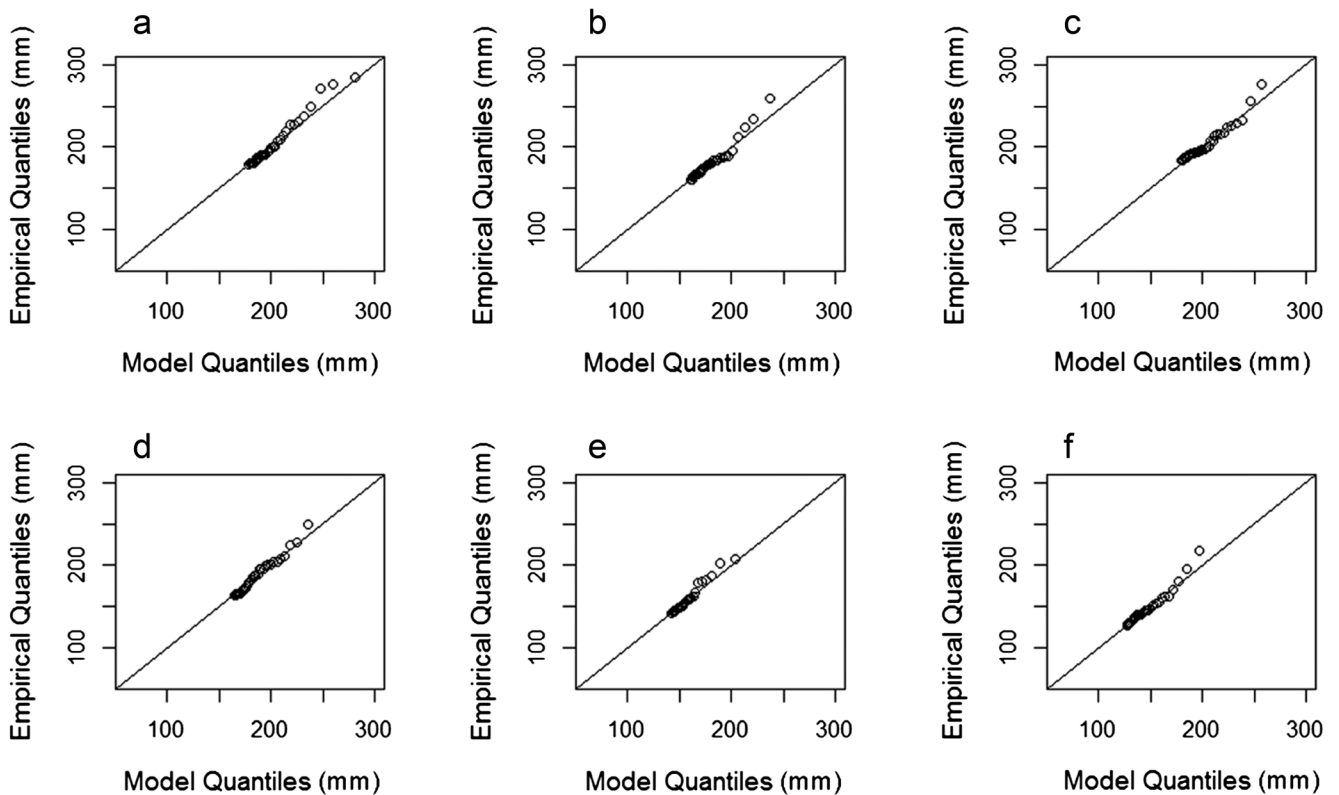

Fig. 7 Quantile–quantile plot for the fit of GPD for homogeneous rainfall regions of the Brazilian Amazon: **a** R1, **b** R2, **c** R3, **d** R4, **e** R5, and **f** R6

Table 2 Results of the Kolmogorov-Smirnov test (at 5 % significance level) to check the quality of fit of the GEV and GPD distributions to the maximum rainfall values for Brazilian Amazon regions with homogeneous rainfall

	GEV		GPD	
	D_n	p value	D_n	p value
R1	0.14	0.55	0.21	0.11
R2	0.18	0.31	0.23	0.06
R3	0.12	0.73	0.21	0.09
R4	0.21	0.11	0.13	0.59
R5	0.15	0.44	0.22	0.08
R6	0.09	0.96	0.20	0.16

4 Conclusions

This work consisted in fitting GEV and GPD distributions to daily precipitation data for the period 1983–2012 in the sub-regions of the Brazilian Amazon with the goal of estimating the return periods of extreme daily precipitation events.

In the GEV distribution, the final datasets used had observations of annual maximum precipitation. For the GPD, we have selected the 0.3 % of the data located in the upper tail of the distribution. The estimate of the parameter of distributions was made by the maximum likelihood method, and the quality of the distributions was graphically evaluated through the quantile–quantile plot. However, the visual analysis of quantile–quantile plot has the disadvantage of being subjective, and for this reason, the non-parametric KS test was also used.

The quantile–quantile plots and non-parametric KS test has shown that the estimates reached by the GEV and GPD were satisfactory. The GEV presents the disadvantage of selecting the extremes by periods/blocks. From each block, a maximum value is extracted. Thus, the maximum within a period may not be, necessarily, an extreme event. However, this method has shown the best fit, relatively to the GPD. Therefore, the GEV and GPD distributions are adequate to study on the maximum and rainfall excesses, respectively.

According to the results of this research work, the highest daily precipitation amounts are expected in the southern region (R1) and at the Amazon coast (R3). It is expected that there will be a daily rainfall total of 152.1 and 164.6 mm at least once a year and a daily total of 251.5 and 234.9 mm at least once every 10 years in the south and at the coast of the Amazon, respectively. The lowest values are expected in the Northwest Amazon (R6); it is expected at least once a year that the daily precipitation over 97.9 mm occurs and a daily total of 175.1 mm at least once every 10 years.

The performed regional analyses of daily precipitation extreme events in the Amazon are expected to contribute to better strategic planning and minimize the risk of loses in productive sectors (particularly in agriculture and electric power generation and distribution).

References

Abild J, Andersen EY, Rosbjerg D (1992) The climate of extreme winds at the Great Belt, Denmark. J Wind Eng Ind Aerodyn 41:521–532. doi:10.1016/0167-6105(92)90458-M

Alcantara CR, Silva Dias MAF, Souza EP, Cohen JCP (2011) Verification of the role of the low level jets in Amazon squall lines. Atmos Res 100:36–44. doi:10.1016/j.atmosres.2010.12.023

An Y, Pandey MD (2005) A comparison of methods of extreme wind speed estimation. J Wind Eng Ind Aerodyn 93:535–545. doi:10.1016/j.jweia.2005.05.003

Bagley JE, Desai AR, Harding KJ, Snyder PK, Foley JA (2014) Drought and deforestation: has land cover change influenced recent precipitation extremes in the Amazon? Journal of Climate 27:345–361. doi:10.1175/JCLI-D-12-00369.1

Barbara F, Hendrik F, Hans-Jürgen P, Gerd S, Daniela J, Philip L, Klaus K (2010) Determination of precipitation return values in complex terrain and their evaluation. Journal of Climate 23:2257–2274. doi:10.1175/2009JCLI2685.1

Bordi I, Fraedrich K, Petitta M, Sutera A (2007) Extreme value analysis of wet and dry periods in Sicily. Theor Appl Climatol 87(1–4):61–71. doi:10.1007/s00704-005-0195-3

Carvalho LMV, Jones C, Liebmann B (2004) The South Atlantic Convergence Zone: intensity, form, persistence, and relationships with intraseasonal to interannual activity and extreme rainfall. J Clim 17:88–108. doi:10.1175/1520-0442(2004)017<0088:TSACZI>2.0.CO;2

Carvalho LMV, Jones C, Silva Dias MAF (2002) Intraseasonal large-scale circulations and mesoscale convective activity in tropical South America during the TRMM-LBA campaign. Journal of Geophysical Researches 107(D20): LBA 9-1–LBA 9-20. DOI: 10.1029/2001JD000745

Chakravarti IM, Laha RG, Roy J (1967) In: Handbook of methods of applied statistics, vol Volume I. John Wiley and Sons, pp. 392–394

Coelho CAS, Cavalcanti IAF, Costa SMS, Freitas SR, Ito ER, Luz G, Santos AF, Nobre CA, Marengo JÁ, Pezza AB (2012) Climate diagnostics of three major drought events in the amazon and illustrations of their seasonal precipitation predictions. Meteorol Appl 19:237–255. doi:10.1002/met.1324

Cohen JCP, Silva Dias MAF, Nobre CA (1995) Environmental conditions associated with Amazonian squall lines: a case study. Mon Weather Rev 123:3163–3174. doi:10.1175/1520-0493(1995)123<3163:ECAWAS>2.0.CO;2

Coles S (2001) An introduction to statistical modeling of extreme values. Springer, London 209 pp. doi:10.1007/978-1-4471-3675-0

Da Rocha RP, Morales CA, Cuadra SV, Ambrizzi T (2009) Precipitation diurnal cycle and summer climatology assessment over south America: an evaluation of regional climate model version 3 simulations. J Geophys Res, 114: D10108. DOI:10.1029/2008JD010212

Davison AC, Smith RL (1990) Models for exceedances over high thresholds. Journal of the Royal Statistical Society, B 52:393–442

De Oliveira Vieira S, Satyamurty P, Andreoli RV (2013) On the South Atlantic convergence zone affecting southern Amazonia in austral summer. Atmos Sci Lett 14:1–6. doi:10.1002/asl.401

De Souza EB, Kayano MT, Ambrizzi T (2005) Intraseasonal and submonthly variability over the eastern amazon and northeast Brazil during the autumn rainy season. Theor Appl Climatol 81:177–191. doi:10.1007/s00704-004-0081-4

De Souza EB, Rocha EJP (2006) Diurnal variations of rainfall in Bragança-PA (eastern Amazon) during rainy season: mean characteristics and extreme events. Revista Brasileira de Meteorologia 21(3):142–152

DeGaetano AT (2009) Time-dependent changes in extreme-precipitation return-period amounts in the Continental United States. Journal of

Applied Meteorology and Climatology 48:2086–2099. doi:10.1175/2009JAMC2179.1

Durieux L, Machado LAT, Laurent H (2003) The impact of deforestation on cloud cover over the amazon arc of deforestation. Remote Sens Environ 86:132–140. doi:10.1016/S0034-4257(03)00095-6

Ender M, Ma T (2014) Extreme value modeling of precipitation in case studies for China. International Journal of Scientific and Innovative Mathematical Research (IJSIMR) 2(1):23–36

Fisher RA, Tippett LHC (1928) Limiting forms of the frequency distribution of the largest or smallest member of a sample. Proc Camb Philos Soc 24(2):180–190

Garreaud RD, Wallace JM (1997) The diurnal March of convective cloudiness over the Americas. Monthly Weather Review 125:3157–3171. doi:10.1175/1520-0493(1997)125<3157:TDMOCC>2.0.CO;2

Gloor M, Brienen RJW, Galbraith D, Feldpausch TR, Schöngart J, Guyot J-L, Espinoza JC, Lloyd J, Phillips OL (2013) Intensification of the amazon hydrological cycle over the last two decades. Geophys Res Lett 40:1729–1733. doi:10.1002/grl.50377

Gnedenko B (1943) Sur la distribution limite du terme maximum d'une série aléatoire. The Annals of Mathematics 44(3):423–453

Grimm AM (2011) Interannual climate variability in south America: impacts on seasonal precipitation, extreme events and possible effects of climate change. Stoch Env Res Risk A 25(4):537–554. doi:10.1007/s00477-010-0420-1

Jenkinson AF (1955) The frequency distribution of the annual maximum (or minimum) of meteorological elements. Q J R Meteorol Soc 81:158–171. doi:10.1002/qj.4970813480

Kostopoulo E, Jones PD (2005) Assesment of climate extremes in the eastern mediterrenean. Meteorog Atmos Phys 89:69–85. doi:10.1007/s00703-005-0122-2

Langerwisch F, Rost S, Gerten D, Poulter B, Rammig A, Cramer W (2013) Potential effects of climate change on inundation patterns in the Amazon Basin. Hydrol Earth Syst Sci 17:2247–2262. doi:10.5194/hess-17-2247-2013

Li Y, Cai W, Campbell EP (2005) Statistical modeling of extreme rainfall in Southwest Western Australia. Journal of Climate 18:852–863. doi:10.1175/JCLI-3296.1

Lucio PS (2004) Assessing HadCM3 simulations from NCEP reanalyses over Europe: diagnostics of block-seasonal extreme temperature s regimes. Glob Planet Chang 44:39–57. doi:10.1016/j.gloplacha.2004.06.004

Maraun D, Rust HW, Osborn TJ (2009) The annual cycle of heavy precipitation across the United Kingdom: a model based on extreme value statistics. Int J Climatol 29:1731–1744. doi:10.1002/joc.1811

Marengo JA, Alves LM, Soares WR, Rodriguez DA, Camargo H, Riveros MP, Pabló AD (2013) Two contrasting severe seasonal extremes in tropical south America in 2012: flood in Amazonia and drought in northeast Brazil. J Clim 26:9137–9154. doi:10.1175/JCLI-D-12-00642.1

Marengo JA, Liebmann B, Grimm AM, Misra V, Silva Dias PL, Cavalcanti IFA, Carvalho LMV, Berbery EH, Ambrizzi T, Vera CS, Saulo AC, Nogues-Paegle J, Zipser E, Seth A, Alves LM (2012a) Recent developments on the South American monsoon system. Int J Climatol 32:1–21. doi:10.1002/joc.2254

Marengo JA, Nobre CA (2009) Clima na região amazônica. In: Cavalcanti IFA, Ferreira NJ, Justi da Silva MGA, Silva Dias MAF (eds) Tempo e Clima no Brasil. Oficina de Textos, São Paulo, Brazil, pp. 197–212

Marengo JA, Nobre CA, Tomasella J, Cardoso MF, Oyama MD (2008a) Hydro-climatic and ecological behaviour of the drought of Amazonia in 2005. Philos Trans R Soc Lond 363:1773–1778. doi:10.1098/rstb.2007.0015

Marengo JA, Nobre CA, Tomasella J, Oyama MD, Oliveira GS, Oliveira R, Camargo H, Alves LM, Brown F (2008b) The drought of Amazonia in 2005. J Clim 21(3):495–516. doi:10.1175/2007JCLI1600.1

Marengo JA, Tomasella J, Alves LM, Soares WR, Rodriguez DA (2011) The drought of 2010 in the context of historical droughts in the amazon region. Geophys Res Lett 38, L12703, DOI:10.1029/2011GL047436

Marengo JA, Tomasella J, Soares WR, Alves LM, Nobre CA (2012b) Extreme climatic events in the Amazon Basin: climatological and hydrological context of previous floods. Theor Appl Climatol 107:73–85. doi:10.1007/s00704-011-0465-1

Nadarajah S, Choi D (2007) Maximum daily rainfall in South Korea. Journal of Earth System Science 116(4):311–320

Nobre CA, Sellers PJ, Shukla J (1991) Amazonian deforestation and regional climate change. J Clim 4(10):957–988. doi:10.1175/1520-0442(1991)004<0957:ADARCC>2.0.CO;2

Oliveira AP, Fitzjarrald DR (1993) The amazon river breeze and the local boundary layer: I - observarions. Boundarry Layer Meteorology 63:141–162. doi:10.1007/BF00705380

Palutikof JP, Brabson BB, Lister DH, Adcock ST (1999) A review of methods to calculate extreme wind speeds. Meteorol Appl 6(2):119–132. doi:10.1017/S1350482799001103

Pickands J (1975) Statistical inference using extreme order statistics. Annals of Statistics, Hayward 3(1):119–131

Rao VB, Hada K (1990) Characteristcs of rainfall over Brazil annual variations and connections with the southern oscillation. Theor Appl Climatol 42:81–91. doi:10.1007/BF00868215

Reboita MS, Gan MA, Rocha RP, Ambrizzi T (2010) Regimes de precipitação na américa do Sul: uma revisão bibliográfica. Revista Brasileira de Meteorologia 25:185–204

Santos EB, Lucio PS, Santos e Silva CM (2014) Precipitation regionalization of the Brazilian amazon. Atmos Sci Lett. doi:10.1002/asl2.535

Sena JA, Beser de Deus LA, Freitas MAV, Costa L (2012) Extreme events of droughts and floods in Amazonia: 2005 and 2009. Water Resour Manag 26:1665–1676. doi:10.1007/s11260-012-9978-3

Sharma P, Khare M, Chakrabarti SP (1999) Application of extreme value theory for predicting violations of air quality standards for an urban road intersection. Transp Res Part D: Transp Environ 4(3):201–216. doi:10.1016/S1361-9209(99)00006-1

Silva Dias MAF, Silva Dias PL, Longo M, Fitzjarrald DR, Denning AS (2004) River breeze circulation in eastern Amazonia: observations and modeling results. Theor Appl Climatol 78:111–121. doi:10.1007/s00704-004-0047-6

Smith JA, Baeck ML, Steiner M, Miller AJ (1996) Catastrophic rainfall from an upslope thunderstorm in the central Appalachians: the rapidan storm of June 27. Water Resour Res 32(10):3099–3113. doi:10.1029/96WR02107

Smith RL (1985) Maximum likelihood estimation in a class of nonregular cases. Biometrika 72:67–90

Sugahara S, da Rocha RP, Silveira R (2009) Non-stationary frequency analysis of extreme daily rainfall in Sao Paulo, Brazil. Int J Climatol 29:1339–1349. doi:10.1002/joc.1760

Vale R, Filizola N, Souza R, Schongart J (2011) A cheia de 2009 na Amazônia Brasileira. Revista Brasileira de Geociências [online]. 41(4):577–586. ISSN 0375–7536

Withers CS, Nadarajah S (2000) Evidence of trend in return levels for daily rainfall in New Zealand. Journal of Hydrology (NZ) 39(2):155–166

Zhou J, Lau K-M (1998) Does a monsoon climate exist over South America? J Clim 11:1020–1040. doi:10.1175/1520-0442(1998)011<1020:DAMCEO>2.0.CO;2